Stress- and Strain-Induced Formation of Martensite and Its Effects on Strength and Ductility of Metastable Austenitic Stainless Steels

DIETER FAHR

The effects of deformation-induced formation of martensite have been studied in metastable austenitic stainless steels. The stability of the austenite, being the critical factor in the formation of martensite, was controlled principally by varying the amounts of carbon and manganese. The formation of martensite was also affected by different test and rolling temperatures, rolling time, and various reductions in thickness. The terms "stress-induced" and "strain-induced" formation of martensite are defined. Experimental results show that low austenite stability resulted in stress-induced formation of martensite, high work-hardening rates, high tensile strengths, low "yield strengths," and low elongation values. When the austenite was stable, plastic deformation was initiated by slip, and the work-hardening rate was too low to prevent early necking. A specific amount of strain-induced martensite led to an "optimum" work-hardening rate, resulting in high strength *and* high ductility. For best results processing should be carried out above M_d and testing between M_d and M_s. Mechanical working above M_d had a negligible effect on the yield strength between M_d and M_s when the austenite stability was low, but its effect increased as the austenite became more stable. Serrations appeared in the stress-strain curve when martensite was strain induced.

UNUSUALLY high strengths can be imparted to many steels through special heat treatments or by combined thermal and mechanical treatments. Most ultrahigh strength steels undergo an austenite-martensite phase transformation, so that at least a portion of their strength is due to a transformation product of low ductility which often limits the application of such steels.

Austenitic steels can be significantly strengthened without a concomitant phase transformation through heavy working in combination with precipitation hardening. The low elongation values observed for these steels during tensile testing are due to a local plastic instability which occurs because the material is unable to work harden at a rate high enough to compensate for the stress increase due to the reduction in cross sectional area. Increasing the ductility in high-strength austenitic steels thus becomes a problem of increasing the work-hardening rate. This can be achieved through a deformation-induced phase transformation. Bressanelli and Moskowitz[1] studied the combined and individual effects of composition, test temperature, and deformation rate on the tensile properties of type 301 stainless steel and clearly demonstrated the beneficial effect of a "specific amount of martensite formation" on tensile elongation. In recent years this deformation-induced formation of martensite was successfully utilized to enhance the ductility of high-strength metastable austenitic stainless steels.[2]

When the free energy difference between martensite and austenite, $\Delta F = F_M - F_A$, reaches a critical negative value, martensite starts forming spontaneously on cooling at the M_s temperature. Since the martensite transformation is a diffusionless shear transformation aided by positive normal stresses,[3,4] it can be made to occur at temperatures above M_s by deformation of the austenite. Above a certain temperature, M_d, no deformation-induced transformation is possible.

Between the M_s and M_d temperatures the formation of martensite can be induced by elastic[3-5] and/or plastic[6-14] deformation. Within this temperature interval the driving force for the reaction consists of 1) the free energy difference, ΔF, between the martensitic and austenitic states, and 2) the externally applied stress. As the difference between F_A and F_M increases with decreasing temperature, lower applied stresses are needed to form martensite. At temperatures near M_s the stress required for slip in the austenitic matrix exceeds that necessary for the martensitic transformation. Conversely, as the temperature increases toward the M_d temperature the stress required for martensite formation increases to a level above that required for slip in the austenite.

In analogy to "stress aging" and "strain aging",[15,16] the author proposes therefore to distinguish between "stress-induced" and "strain-induced" formation of martensite. Martensite is considered to be "stress induced" when it forms as a result of elastic stresses from an external load (*i.e.*, below the actual yield strength of the austenite). The condition for stress-induced formation of martensite is therefore $\sigma_{A \rightarrow M} < \sigma_{\text{yield}\,A}$. Martensite is "strain induced" when slip in the austenite precedes its formation. Strain-induced martensite, thus, forms only when $\sigma_{A \rightarrow M} > \sigma_{\text{yield}\,A}$.

The rate of martensite formation upon straining a metastable austenitic steel depends on the stability of the austenite. For a given deformation temperature the austenite stability is a function of the alloy content

DIETER FAHR, formerly Graduate Student, Department of Materials Science and Engineering, University of California, Berkeley, Calif., is now with the Metals and Ceramics Division, Oak Ridge National Laboratory, Oak Ridge, Tenn.

Manuscript submitted October 2, 1970.

and the thermomechanical history. The addition of almost any element, with the possible exception of cobalt, increases the austenite stability with respect to the formation of martensite either spontaneously or by deformation (*i.e.*, suppresses the M_s and M_d temperatures, independent of whether or not the added element has an fcc lattice structure). Austenite of a given composition can be further stabilized by mechanical and/or thermal treatments. Large amounts of deformation of the austenite increase its dislocation density and thus make the cooperative movement of atoms during formation of martensite more difficult. Moreover, the volume of the martensite is larger (approximately 4 pct) than that of the austenite from which it forms.[4] This volume increase must be accommodated by the generation and motion of dislocations in the austenite. A high dislocation density in the austenite makes this more difficult. Thermal treatments allow interstitial atoms to lock mobile dislocations and thus increase the austenite stability for the same reason. Prior transformation has an effect similar to plastic deformation on the austenite stability. If a steel is partially transformed to martensite, the remaining austenite is more difficult to transform and this stability of the austenite is increased even more by aging.

The austenite stability is lowered chemically when thermomechanical treatments lead to extensive precipitation of alloy carbides.[17] The austenite matrix becomes depleted of carbon and alloying elements and the M_s and M_d temperatures increase. Small amounts of plastic deformation tend to promote the formation of martensite in ferrous alloys with a low stacking fault energy.[18] Several investigators[11,18,19] have suggested that strain-induced stacking faults may play a role in the nucleation of the martensite, but local stress concentrations are generally believed to be the primary martensite nucleation sites.

This investigation was conducted to determine the conditions for an optimum balance of high strength and ductility when martensite is forming during the test. Since the austenite stability plays an all-important role, alloys with varying manganese and carbon contents were processed and tested at different temperatures and reduced from 20 to 80 pct in thickness.

EXPERIMENTAL PROCEDURE

Alloy Preparation

The alloys listed in Table I were prepared by induction melting commercially pure (99.9 pct) elements in an argon atmosphere. The resulting 20-lb. ingots were homogenized for three days at 1050°C, forged at 1100°C to break up the cast structure, and then reduced by rolling at 450°C. This was followed by an austenitizing treatment of 1 hr at 1200°C in a helium atmosphere.

Table II lists the thermomechanical treatments applied to the as-austenitized alloys. The samples were reheated to the rolling temperature between passes.

Specimen Preparation and Testing

Tensile specimens with a gage length of 1 in. and a width of 0.125 in. were ground from 0.050 in. sheet. Tensile tests were conducted at four different temperatures using an Instron Testing Machine at a crosshead speed of 0.04 in. per min. Tests were performed at room temperature in air, at 100°C in boiling distilled water, at −78°C in dry ice and ethanol, and at −196°C in a liquid nitrogen bath.

Table I. Composition of Steels Examined

Heat Number	Composition*, wt pct			
	Cr	Ni	Mn	C
692-9	9.0	8.0 (7.6)	1.0	0.2 (0.21)
692-7	9.0	8.0	1.0	0.3 (0.29)
6811-15	9.0 (10.1)	8.0 (7.6)	1.0	0.4 (0.43)
689-18	9.0 (10.3)	8.0	1.0	0.5 (0.53)
6811-14	9.0 (10.1)	8.0 (7.6)	2.0	0.0 (0.01)
6811-13	9.0 (10.1)	8.0 (7.6)	2.0 (2.2)	0.1 (0.17)
6811-12	9.0 (10.7)	8.0 (7.7)	2.0	0.2 (0.28)
689-15	9.0 (9.8)	8.0	2.0	0.3 (0.32)
689-16	9.0 (10.2)	8.0	2.0	0.4 (0.35)
686-21	9.0 (9.2)	8.0 (7.8)	2.0 (2.3)	0.5 (0.51)
692-8	9.0	8.0	3.0	0.2 (0.25)
6812-11	9.0 (10.1)	8.0 (7.7)	3.0	0.3 (0.34)
692-6	9.0	8.0	3.0 (3.4)	0.4 (0.42)
686-22	9.0	8.0 (7.8)	3.0 (3.2)	0.5 (0.52)
689.19	9.0 (10.0)	8.0	4.0	0.5 (0.51)

*Actual values are given in parentheses for carbon and for the other elements when deviation from intended value was greater than ±0.1 wt pct.

Table II. Thermomechanical Treatments Applied to the As-Austenitized Alloys

Reduction in Thickness, Pct	Rolling Temperature, °C
20	450
40	450
60	450
80	450
80	250
80	100
80	24

EXPERIMENTAL RESULTS AND DISCUSSION

Only a few of the many stress-strain curves obtained are presented in this paper. They show the typical features associated with stress- and strain-induced formation of martensite during a tensile test as a function of the variables investigated.

Whenever a well-defined yield point was observed, the upper yield point was taken as the yield criterion; otherwise, the 0.2 pct offset yield strength was used.

Stress- and strain-induced martensite were distinguished on the basis of yield strength. When the yield strength at room temperature was less than at 100°C, it was concluded that stress-induced formation of martensite initiated plastic deformation at room temperature. The same reasoning applied to results obtained at lower temperatures. Quotation marks are used to distinguish between the onset of plastic deformation due to the formation of martensite ("yielding," "yield strength") and the conventional yielding (yield strength) in the absence of a phase transformation.

Whenever the formation of martensite is stress induced, slip in the austenite is a consequence of the formation of martensite. Strain-induced formation of

Fig. 1—Optical photomicrograph of the microstructure of Alloy 689-15 after 80 pct reduction in thickness at room temperature showing deformation markings in an austenitic grain that is surrounded by deformation-induced martensite. Electropolished (90 pct/10 pct acetic/perchloric acid solution at 0°C and 20 V) and etched (5 g cupric chloride, 100 ml hydrochloric acid, 100 ml methyl alcohol, and 100 ml distilled water).

martensite, on the other hand, is itself a consequence of slip in the austenite.

Fig. 1 shows deformation markings in an austenitic grain surrounded by martensite. Since that sample was fully austenitic at room temperature after cooling from 1200°C, both the martensite and the deformation markings were due to the deformation process at room temperature. As a matter of fact, formation of martensite and slip in the austenite compete with one another as modes of deformation.[17] This competition is revealed in serrations in the stress-strain curves when the martensite is strain induced. While the strain-induced martensite forms intermittently resulting in bursts of transformation (serrations), stress-induced martensite does not cause any serrations in the stress-strain curves; it forms so readily that externally applied stresses are sufficient to sustain the phase transformation. Fig. 2 shows the surface relief of stress-induced martensite.

Effect of Alloying Elements

Manganese and carbon were chosen as compositional variables because relatively small additions of these elements lower the M_s and M_d temperatures significantly.[7,8,17,20-22]

Fig. 2—Optical photomicrograph of stress-induced martensite revealed by its surface relief. Direction of applied stress is indicated by arrows. (Alloy 6811-15 after 80 pct reduction in thickness at 250°C.) Electropolished (90 pct/10 pct acetic/perchloric acid solution at 0°C and 20 V).

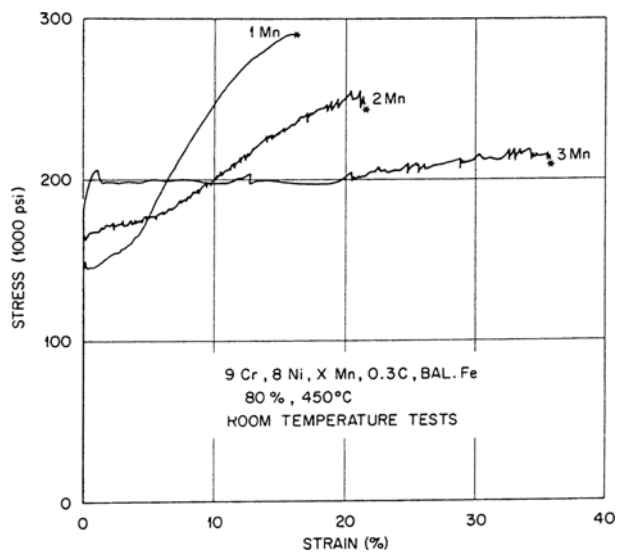

Fig. 3—Effect of varying manganese contents on room-temperature engineering stress-strain curves of 0.3 pct C alloys after 80 pct reduction in thickness at 450°C. Crosshead speed: 0.04 in. per min.

Fig. 3 shows the room-temperature engineering stress-strain curves of the 0.3 pct C alloys containing 1, 2, and 3 pct Mn. The room-temperature tensile data are compared with those obtained at 100°C in

Table III. Tensile Properties* of 0.3% C Steels† with Varying Manganese Contents

Alloy Number	Manganese Content, pct	Reduction in Thickness, pct	Temperature, °C		Strength, psi		Elongation, pct
			Rolling	Test	Yield	Tensile	
					X 10^3	X 10^3	
692-7	1	80	450	24	150	289	16.0
				100	206	212	3.0
689-15	2	80	450	24	166	255	21.5
				100	176	182	0.5
6812-11	3	80	450	24	206	219	35.0
				100	195	201	3.0

*Crosshead speed: 0.04 in. per min. Tested in air at 24°C, in distilled water at 100°C.

†Nominal composition, pct: 9 Cr, 8 Ni, *x* Mn, *y* C, bal Fe.

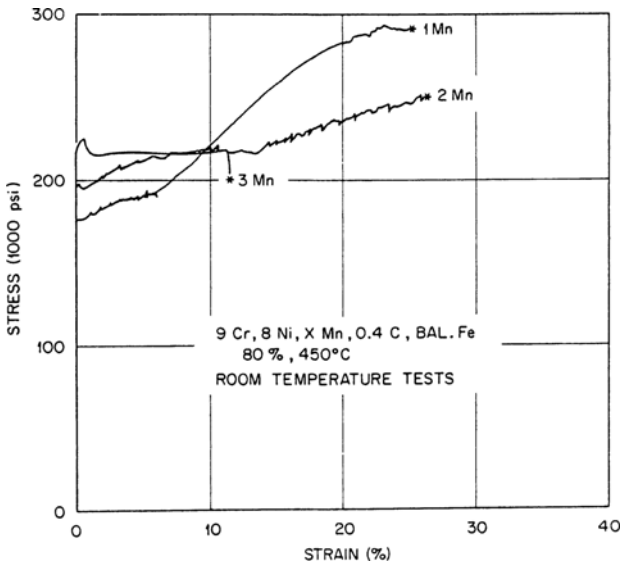

Fig. 4—Effect of varying manganese contents on room-temperature engineering stress-strain curves of 0.4 pct C alloys after 80 pct reduction in thickness at 450°C. Crosshead speed: 0.04 in. per min.

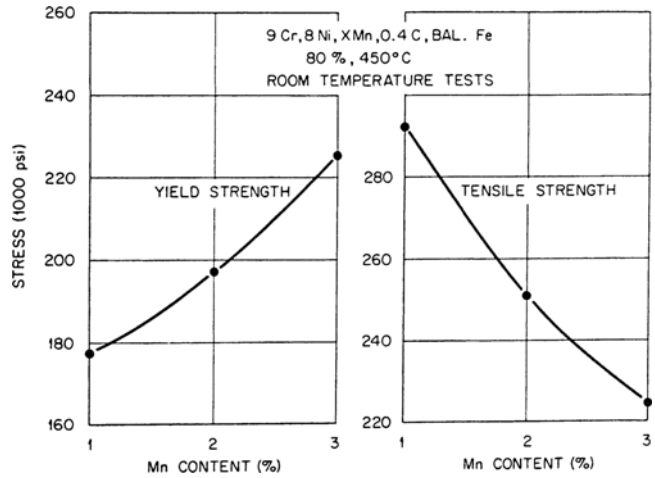

Fig. 5—Effect of increasing manganese content (increasing austenite stability) on room-temperature yield strength and tensile strength, respectively.

Table IV. Tensile Properties* of 0.4% C Steels† with Varying Manganese Contents

Alloy Number	Manganese Content, pct	Reduction in Thickness, pct	Temperature, °C		Strength, psi		Elongation, pct
			Rolling	Test	Yield	Tensile	
					X 10^3	X 10^3	
6811-15	1	80	450	24	177	293	25.0
				100	210	217	2.0
689-16	2	80	450	24	197	251	26.0
				100	200	202	0.5
692-16	3	80	450	24	223	225	11.0
				100	217	225	1.5

*Crosshead speed: 0.04 in. per min. Tested in air at 24°C, in distilled water at 100°C.

†Nominal composition, pct: 9 Cr, 8 Ni, *x* Mn, *y* C, bal Fe.

Table III. The "yield strengths" of the 1 and 2 pct Mn alloys were 56,000 and 10,000 psi lower at room temperature than at 100°C indicating that stress-induced formation of martensite initiated plastic deformation at room temperature in these two alloys. Slip in the austenite was responsible for the onset of plastic deformation in the alloy with 3 pct Mn. Increasing the manganese content resulted in a more stable austenite, and thus in higher yield strength and elongation values and lower work-hardening rates and tensile strengths. The same effects were observed for 0.4 pct C alloys, Figs. 4 and 5, except that the higher carbon content itself led to a higher initial austenite stability, which in turn reduced the difference in yield strength between the 100°C and room-temperature tests of the 1 and 2 pct Mn alloys to 33,000 and 3000 psi, respectively, Table IV. While plastic deformation in these two alloys began as a result of stress-induced formation of martensite, yielding occurred by slip in the austenite in the more stable 3 pct Mn alloy. As in the 0.3 pct C alloys, increasing the manganese content increased the yield strengths and lowered the work-hardening rates and tensile strengths. The elongation, however, first increased and then dropped off rapidly with increasing austenite stability, Fig. 6. Apparently not enough martensite formed in the 3 pct Mn alloy to prevent necking at larger strains. The 3 pct Mn-0.3 pct C alloy displayed a work-hardening rate that was near the optimum (for maximum elongation), whereas that observed for the 3 pct Mn-0.4 pct C alloy was obviously below the optimum rate, Fig. 6. Any further increase in austenite stability (*e.g.*, through higher alloy content) would result in even lower work-hardening rates and elongation values. The stress-strain curves in Fig. 7 show that a 3 pct Mn-0.5 pct C alloy had indeed a lower elongation value than the alloys with less carbon, and that the work-hardening rates increased with decreasing carbon content (decreasing austenite stability). The elongation values increased because more martensite formed upon straining, and thus prevented early necking. As soon as the work-hardening rate exceeded its optimum value, the elongation values decreased again, Fig. 8, since the ultimate tensile strength and the fracture strength of the respective alloys were reached more rapidly (*i.e.*, at less strain). The stress-strain curve of the 0.2 pct C alloy in Fig. 7 shows this very clearly. The lower austenite stability of this alloy is further documented by the lower "yield point." "Yielding" began as a result of stress-induced formation of martensite while the alloys with higher carbon contents yielded by slip in the

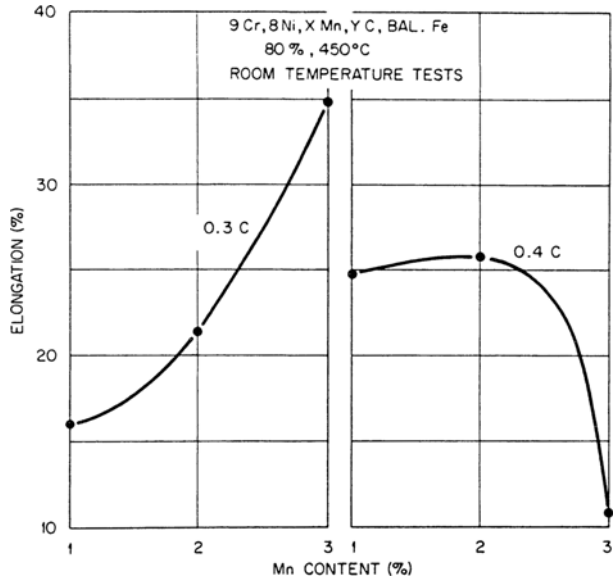

Fig. 6—Effect of increasing manganese content on room-temperature elongation values in alloys with different carbon contents (different austenite stabilities).

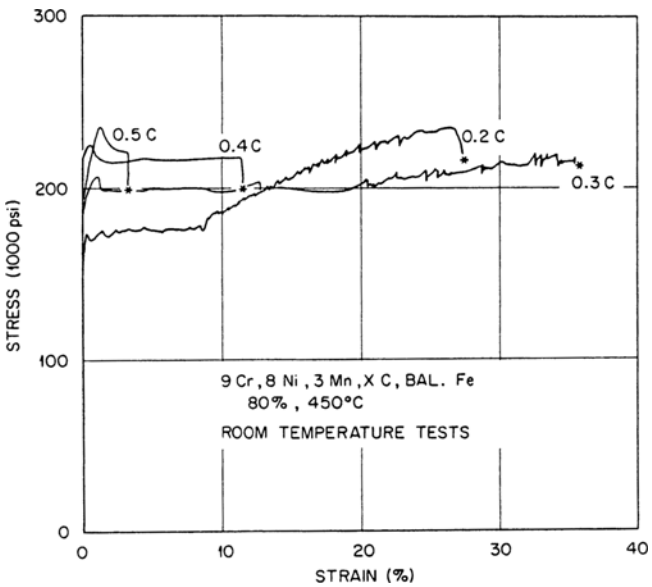

Fig. 7—Effect of varying carbon contents on room-temperature engineering stress-strain curves of 3 pct Mn alloys after 80 pct reduction in thickness at 450°C. Crosshead speed: 0.04 in. per min.

austenite. The initial mode of plastic deformation also seems to affect the appearance of the yield points. Slip apparently resulted in a larger difference between upper and lower yield points than did formation of martensite.

The increase in yield strength with increasing carbon content, Fig. 7, for the higher carbon alloys was not related to the austenite stability. The austenite was stable enough for yielding to occur by slip, but it was due to the different carbon content and its effect on strengthening mechanisms (such as precipitation and solid-solution hardening) during processing at 450°C.

The stress-strain curves in Fig. 7 and other data obtained during this investigation strongly suggest

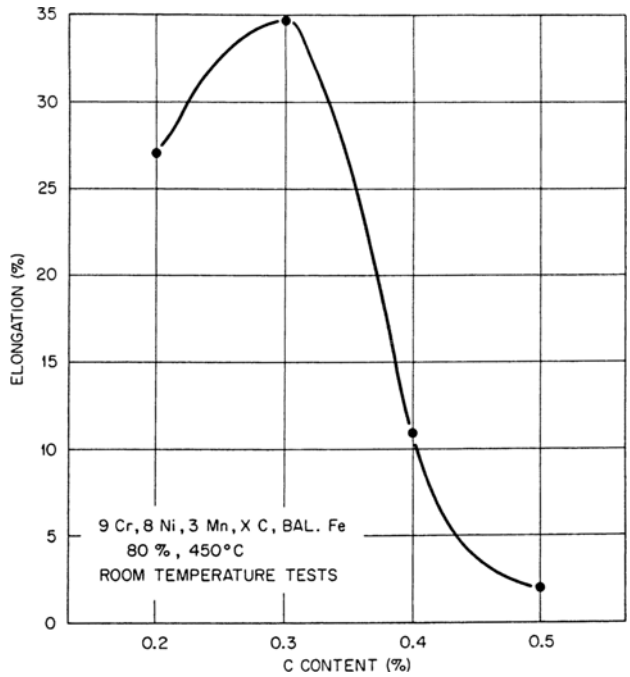

Fig. 8—Effect of increasing carbon content (increasing austenite stability) on the room-temperature elongation values of 3 pct Mn alloys.

that maximum elongation cannot be obtained whenever the austenite stability is such that initial plastic deformation is due to stress-induced formation of martensite. Work-hardening rates will always be higher than the optimum in such a case. Thus, the condition set forth for strain-induced formation of martensite must be met in order to obtain an optimum work-hardening rate.

The strong effect of austenite stability on mechanical properties and its susceptibility to compositional changes is underlined by the fact that differences in carbon content of only 0.1 pct could cause changes in elongation by a factor of more than 3 at stress levels above 200,000 psi. Another variable that affects the austenite stability strongly is the test temperature.

Effect of Test Temperature

Test temperatures ranged from −196° to 100°C, and thus allowed a complete study of the effects of the austenite stability on tensile properties. Since the M_d temperatures of most of the alloys were below 100°C, no phase transformation could be induced at that temperature. This was reflected in the mechanical properties. The work-hardening rate of the austenite was too low to prevent failure at the site of incipient necking. The low ductility obtained for most alloys in liquid nitrogen tests was due to the martensite that formed spontaneously on cooling to −196°C ($M_s > -196$°C). The elongation test-temperature curve in Fig. 9 shows how the ductility can be optimized when tests are carried out between these two extremes (*i.e.*, between M_s and M_d). It also indicates the approximate temperature (close to M_d) where the rate of formation of martensite led to an optimum work-hardening rate, and thus to maximum elongation.

Fig. 10 shows the variation of "yield strength" with test temperature for a relatively unstable alloy.

Stress-induced formation of martensite was responsible for the decrease in "yield strength" as the test temperature was lowered. Spontaneous formation of martensite on cooling to −196°C effectively strengthened the remaining austenite. This explains why the "yield strength" at −196°C is higher than at −78°C.

The stress-strain curves in Fig. 11 are representative of alloys with different austenite stabilities. Three cases are described. The work-hardening rates at room temperatures are 1) higher, Fig. 11(*a*), 2) approximately at, Fig. 11(*c*), and 3) lower, Fig. 11(*e*), than the optimum work-hardening rate. In the first case, more martensite formed than was required to prevent necking, and in the last case, a 4 pct Mn alloy was tested to ensure that no martensite formed at all. The much lower austenite stability at −78°C as compared to room temperature is reflected in the stress-strain curves of Figs. 11(*b*), (*d*), and (*f*). The work-hardening rates were drastically increased, thus lowering elongation for the alloys that had work-hardening rates at or above the optimum at room temperature, and increasing it for the alloy whose work-hardening rate was below the optimum at 24°C. The 4 pct Mn alloy, Figs. 11(*e*) and (*f*), demonstrated impressively the effect of test temperature on the austenite stability, and thus on the mechanical properties. The stability of the austenite is also affected by the various processing variables.

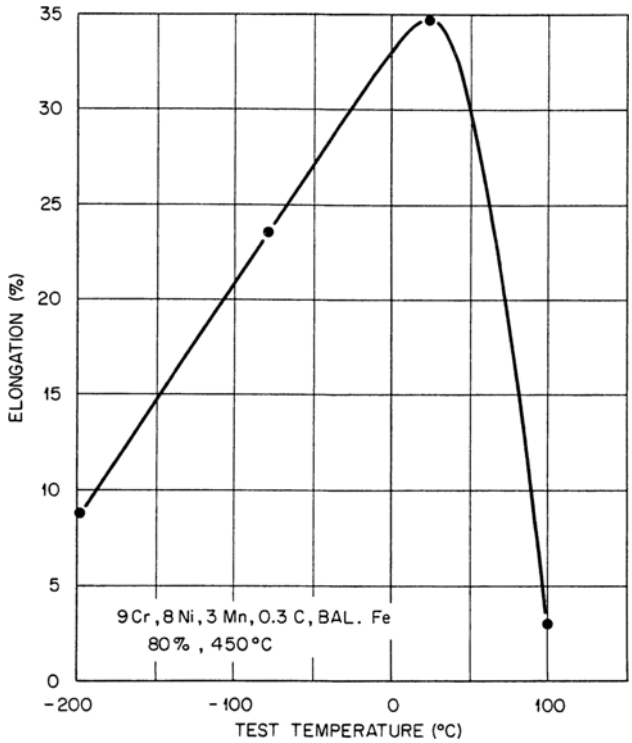

Fig. 9—Variation of elongation values with test temperature (austenite stability).

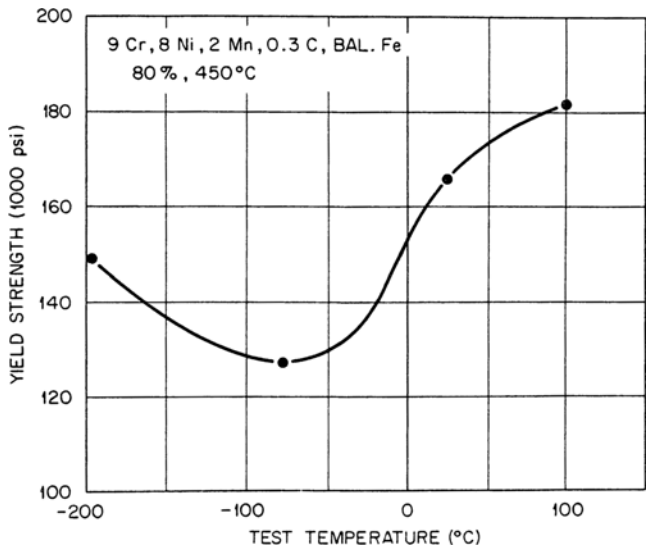

Fig. 10—Variation of "yield strength" values with test temperature.

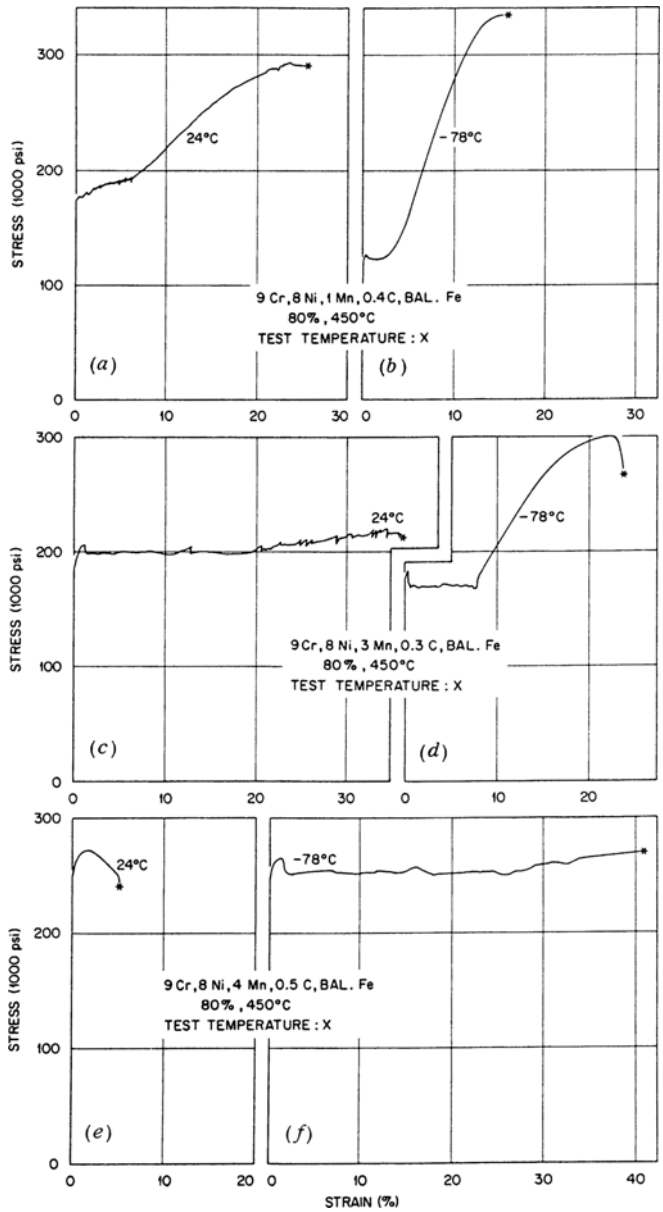

Fig. 11—Comparison of effects of different test temperatures (24° and −78°C) on the shape of the engineering stress-strain curves of alloys with different austenite stabilities. Crosshead speed: 0.04 in. per min.

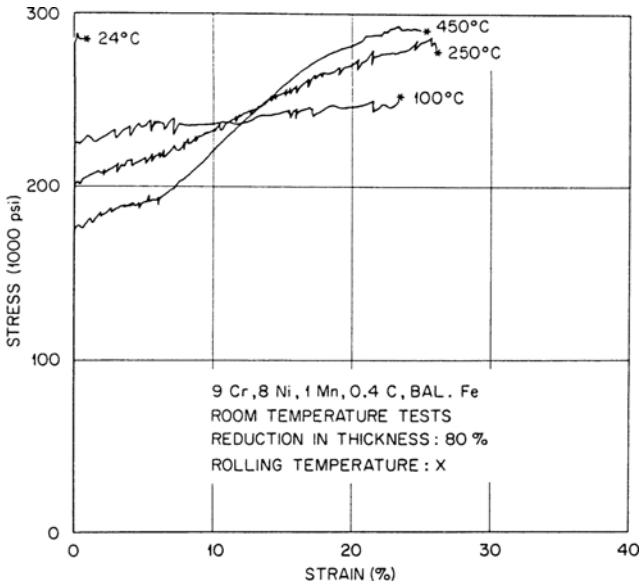

Fig. 12—Effect of different rolling temperatures (different austenite stabilities) on the room-temperature engineering stress-strain curves.

Effects of Processing Variables

Depending on the stability of the austenite, formation of martensite could be observed: 1) on cooling from the austenitizing temperature (1200°C) to room temperature ($M_s > RT$), 2) during rolling at room temperature ($M_d > RT$), 3) during cooling to test temperatures below room temperature, and finally 4) during the tensile test itself.

Rolling Temperature

The rolling temperature affected the pretest austenite stability in two ways: 1) chemically by the precipitation process at higher rolling temperature, and 2) mechanically by the formation of martensite during rolling at lower temperatures (*i.e.*, the retained austenite became more stable).

This effect of rolling temperature is illustrated in Fig. 12, which shows room-temperature stress-strain curves after 80 pct reduction in thickness at 24°, 100°, 250°, and 450°C, respectively. Formation of martensite during rolling at room temperature resulted in high yield strength and low ductility. The specimens rolled at higher temperatures were fully austenitic before the test, and "yielding" was initiated by stress-induced formation of martensite. Table V lists the room-temperature and 100°C tensile properties, and it can be seen that the difference in "yield strength" between room temperature and 100°C tests increased with increasing rolling temperature. Higher temperatures led to increased precipitation, and thus to a lower austenite stability. Yield strengths, work-hardening rates, and tensile strengths reflected the marked effect of the rolling temperature on the austenite stability, Fig. 12.

Amount of Reduction During Rolling and Rolling Time

Rolling above the M_d temperature hardly affected the yield strength between M_d and M_s when "yielding"

Table V. Tensile Properties* of Alloy 6811-15†

Reduction in Thickness, pct	Temperature, °C		Strength, psi		Elongation, pct
	Rolling	Test	Yield	Tensile	
			X 10^3	X 10^3	
80	24	24	289		0.5
		100	281‡		0.0
80	100	24	226	251	23.5
		100	227‡		0.0
80	250	24	203	286	26.0
		100	233	236	2.0
80	450	24	177	293	25.0
		100	214	217	2.0

*Crosshead speed: 0.04 in. per min. Tested in air at 24°C, in distilled water at 100°C.
†Nominal composition, pct: 9 Cr, 8 Ni, 1 Mn, 0.4 C, bal Fe.
‡Fracture strength.

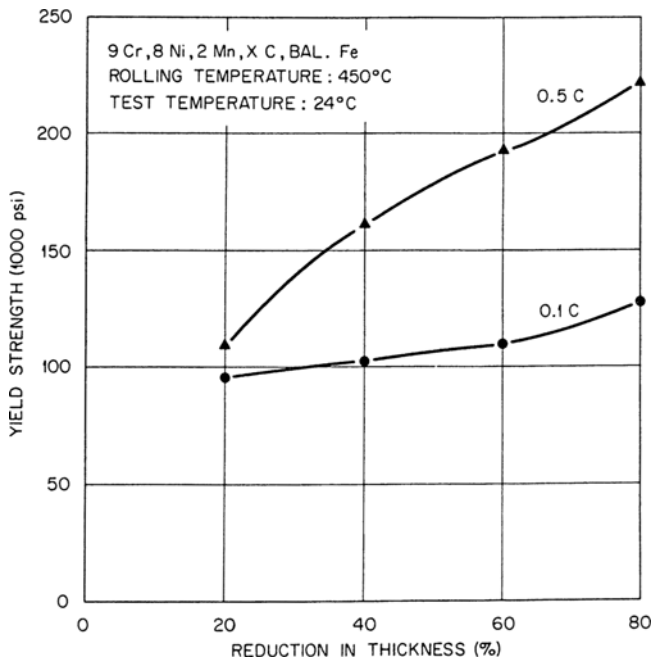

Fig. 13—Effect of prior deformation at 450°C ($> M_d$) on the room-temperature ($< M_d$) yield strength of alloys with high (0.5 pct C) and low (0.1 pct C) austenite stabilities.

began as a result of stress-induced formation of martensite. The yield-strength versus reduction-in-thickness curves in Fig. 13 show that the effect of prior cold work on the yield strength increased with increasing carbon content (higher austenite stability).

The prior deformation at 450°C affected the austenite stability in several ways. Large reductions in thickness tend to stabilize the austenite mechanically while concurrent precipitation processes decrease the austenite stability chemically. Moreover, larger amounts of plastic deformation at 450°C generally provide more nucleation sites for carbide precipitates and possibly enhance diffusion. Since more time was required for large reductions in thickness, the amount of precipitation increased and the austenite thus became less stable chemically the larger the reduction in thickness at 450°C. The stress-strain curves in Fig. 14 show that the "yield strength" of a specimen with 80 pct reduc-

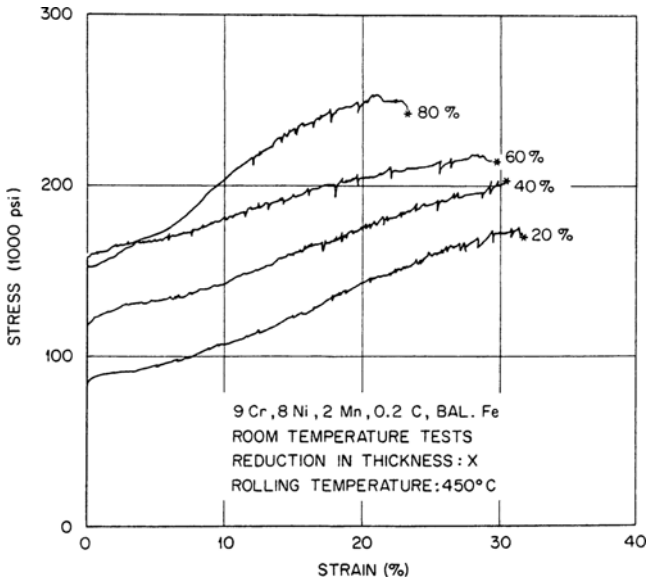

Fig. 14—Effect of varying reductions in thickness (and rolling times) at 450°C on the room-temperature engineering stress-strain curves of a relatively unstable alloy. Crosshead speed: 0.04 in. per min.

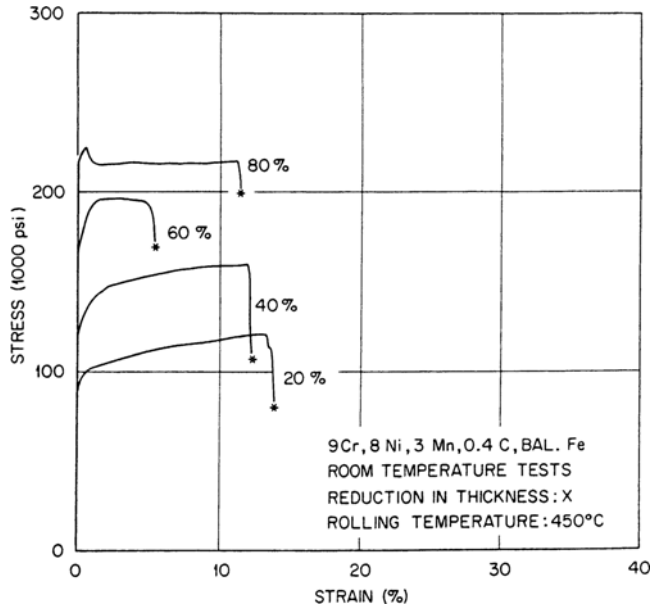

Fig. 15—Effect of varying reductions in thickness (and rolling times) at 450°C on the room-temperature engineering stress-strain curves of a relatively stable alloy. Crosshead speed: 0.04 in. per min.

tion in thickness was actually lower than that of a specimen of the same alloy with only 60 pct prior deformation. This was presumably due to additional precipitation in the specimen with 80 pct reduction since it took twice as much time (60 vs 30 min) to reduce a specimen 80 pct as was required for a 60 pct reduction in thickness at 450°C. The stress-strain curves in Fig. 15 show that the austenite stability is decreased as a result of longer rolling times in a more stable alloy as well. The elongation values decreased with increasing amounts of prior deformation for specimens held for the same length of time at 450°C (20, 40, and 60 pct reduction in thickness). The specimen with 80 pct reduction in thickness at 450°C was dynamically "strain aged" for a longer time, and the austenite thus became less stable. This lower austenite stability resulted in a higher elongation value than in the specimen with 60 pct prior deformation.

To separate the effect of time from that of plastic deformation on the austenite stability, specimens with 60 pct reduction at 450°C (rolling time 40 min) were tested at room temperature in the as-rolled condition and after an additional aging treatment of 80 min at 450°C. The stress-strain curves in Fig. 16 show how the decreased austenite stability of the tempered specimen resulted in an increased work-hardening rate, a higher tensile strength (260,000 vs 240,000 psi), and a lower elongation value (11 vs 16 pct). The microstructures of the untempered and the tempered specimens, as shown in Figs. 17(a) and (b), clearly reveal additional precipitation due to prolonged aging at the rolling temperature. It is assumed that the strengthening effect of the precipitates in the partly transformed specimen ($M_s >$ room temperature; 2 pct Mn-0.1 pct C) and, possibly, further transformation to martensite on cooling from 450°C to room temperature caused the tempered specimen, in spite of its lower austenite stability, to "yield" at the same stress as the untempered specimen.

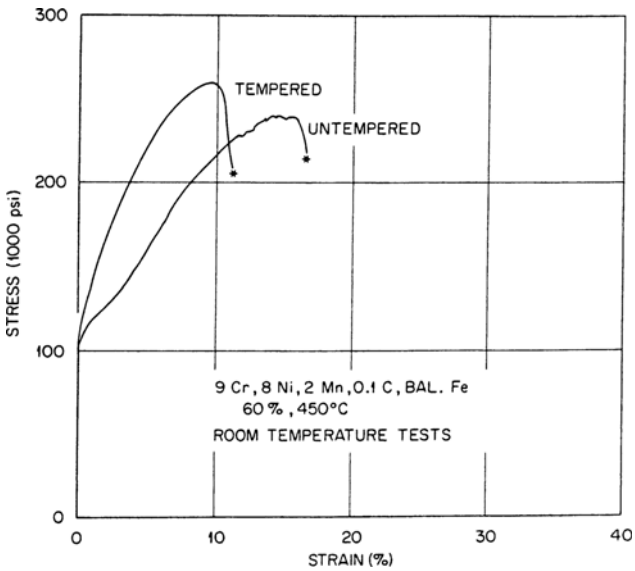

Fig. 16—Effect of annealing (80 min at 450°C) on the room-temperature engineering stress-strain curve of a partially transformed ($M_s > RT$) alloy (Alloy 6811-13). Crosshead speed: 0.04 in. per min.

SUMMARY AND CONCLUSIONS

The deformation-induced formation of martensite in metastable austenitic stainless steels has been studied as a function of manganese and carbon contents, test temperature, and thermomechanical treatment. Conditions under which the ductility of high-strength steels could be improved were of primary interest. The principal results and conclusions can be summarized as follows:

1) The austenite stability controlled the mechanical properties investigated. Variations in manganese and carbon content and changes in test and processing temperatures and the amount of reduction in thickness strongly affected the stability of the austenite.

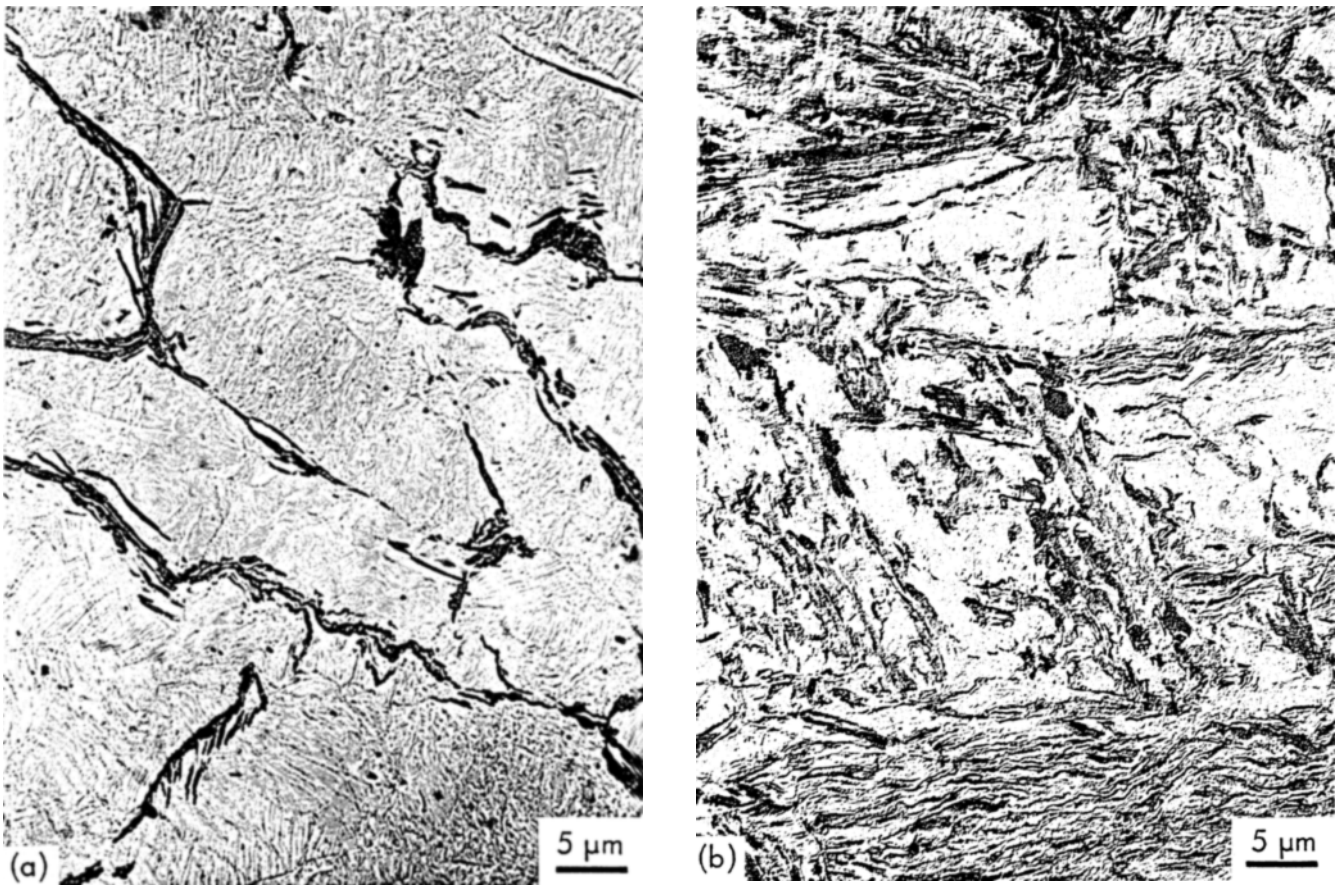

Fig. 17—Optical photomicrograph of the microstructure of Alloy 6811-13 after 60 pct reduction in thickness at 450°C (rolling time: 40 min). (*a*) Untempered; (*b*) tempered (80 min at 450°C). Electropolished (90 pct/10 pct acetic/perchloric acid solution at 0°C and 20 V) and etched (5 g cupric chloride, 100 ml hydrochloric acid, 100 ml methyl alcohol, and 100 ml distilled water).

2) At temperatures between M_s and M_d the martensitic transformation can be "stress" and/or "strain induced." When the stress necessary for martensite formation was lower than that required for slip in the austenite, the transformation was regarded as "stress induced" ($\sigma_{A \rightarrow M} < \sigma_{\text{yield}\,A}$). When slip in the austenite preceded the formation of martensite, the transformation was considered "strain induced" ($\sigma_{A \rightarrow M} > \sigma_{\text{yield}\,A}$).

3) Low austenite stability resulted in low "yield strength" and elongation values, high tensile strengths, and work-hardening rates. With increasing austenite stability, "yield strength" and elongation values increased and tensile strengths and work-hardening rates decreased.

4) The work-hardening rate of stable austenite was found to be inadequate to delay necking at high stress levels.

5) The effect of increasing amounts of prior deformation (above M_d) on the yield strength (between M_d and M_s) was large when the stress required for martensite formation exceeded the yield strength of the austenite. The effect was, however, negligible when the austenite stability was low and the martensite stress induced.

6) When stress-induced formation of martensite initiated plastic deformation, the work-hardening rate of metastable austenite was always higher than the optimum work hardening rate associated with maximum elongation. The combination of high strength *and* high ductility can, therefore, only be obtained at temperatures close to (but below) the M_d temperature (*i.e.*, when slip in the austenite initiates plastic deformation and the formation of martensite is strain induced).

7) Serrations in the stress-strain curves were caused by strain-induced formation of martensite. Slip in the austenite and formation of martensite were regarded as competing modes of plastic deformation. No serrations occurred when the martensite was stress induced.

8) Whenever the formation of martensite is stress induced, slip in the austenite is a consequence of the formation of martensite. Strain-induced formation of martensite, on the other hand, is itself a consequence of slip in the austenite.

9) Test temperatures above M_d (no phase transformation) and below M_s (untempered pretest martensite) led to low elongation values.

10) Rolling at temperatures below M_d (formation of martensite) resulted in "mechanical" stabilization of the remaining austenite. Working at temperatures above M_d provided a less stable austenite because of precipitation. The austenite stability also decreased with increasing (rolling) times at 450°C.

11) The austenite stability has been shown to be significantly affected by small variations in composition and thermomechanical treatment. It also changes

drastically within a relatively narrow temperature range. For these reasons applicability of such metastable austenitic stainless steels is severely limited since both strength and ductility vary with the austenite stability. Application within a small temperature range may be possible only when stringent composition and processing requirements are met.

ACKNOWLEDGMENT

The author wishes to express his appreciation to Profs. Victor F. Zackay and Earl R. Parker of the Department of Materials Science and Engineering, University of California, Berkeley, for their support and encouragement during the course of this investigation. The author is also very grateful to R. W. Carpenter and D. G. Harman of the Metals and Ceramics Division, Oak Ridge National Laboratory, for their helpful comments made on reviewing this paper.

The research was performed in the Inorganic Materials Research Division of the Lawrence Radiation Laboratory, Berkeley, and was supported by the U. S. Atomic Energy Commission.

The manuscript was prepared by the Metals and Ceramics Division Reports Office and the illustrations by the Graphic Arts Department, Oak Ridge National Laboratory.

REFERENCES

1. J. P. Bressanelli and A. Moskowitz: *ASM Trans. Quart.*, 1966, vol. 59, pp. 223-39.
2. V. F. Zackay, E. R. Parker, D. Fahr, and R. Busch: *ASM Trans. Quart.*, 1967, vol. 60, pp. 252-59.
3. S. A. Kulin, M. Cohen, and B. L. Averbach: *Trans. AIME*, 1952, vol. 194, pp. 661-68.
4. J. R. Patel and M. Cohen: *Acta Met.*, 1953, vol. 1, pp. 531-38.
5. E. Scheil: *Z. Anorg. Allgem. Chem.*, 1932, vol. 207, pp. 21-40.
6. B. L. Averbach, S. A. Kulin, and M. Cohen: *Cold Working of Metals*, pp. 290-319, American Society for Metals, 1948.
7. T. Angel: *J. Iron Steel Inst. (London)*, 1954, vol. 177, pp. 165-74.
8. B. Cina: *J. Iron Steel Inst. (London)*, 1954, vol. 177, pp. 406-22.
9. H. C. Fiedler, B. L. Averbach, and M. Cohen: *Trans. Am. Soc. Metals*, 1955, vol. 47, pp. 267-85.
10. B. Cina: *Acta Met.*, 1958, vol. 6, pp. 748-62.
11. J. A. Venables: *Phil. Mag.*, 1962, vol. 7, pp. 35-43.
12. C. J. Guntner and R. P. Reed: *ASM Trans. Quart.*, 1962, vol. 55, pp. 399-419.
13. J. F. Breedis and W. D. Robertson: *Acta Met.*, 1963, vol. 11, pp. 547-59.
14. R. Lagneborn: *Acta Met.*, 1964, vol. 12, pp. 823-43.
15. R. F. Gill, E. A. Smith, and R. H. Harrington: *J. Inst. Metals*, 1950, vol. 78, no. 3, pp. 203-28.
16. R. H. Harrington: *ASM Trans. Quart.*, 1965, vol. 58, pp. 119-41.
17. D. Fahr: Ph.D. Thesis, 1969, University of California, Berkeley, UCRL-19060.
18. H. M. Otte: *Acta Met.*, 1957, vol. 5, pp. 614-27.
19. P. M. Kelly and J. Nutting: *J. Iron Steel Inst. (London)*, 1961, vol. 197, pp. 199-211.
20. K. J. Irvine, D. T. Llewellyn, and F. B. Pickering: *J. Iron Steel Inst. (London)*, 1959, vol. 192, pp. 218-38.
21. K. J. Irvine, F. B. Pickering, and J. Garston: *J. Iron Steel Inst. (London)*, 1960, vol. 196, pp. 66-81.
22. C. B. Post and W. S. Eberly: *ASM Trans. Quart.*, 1947, vol. 39, pp. 868-90.